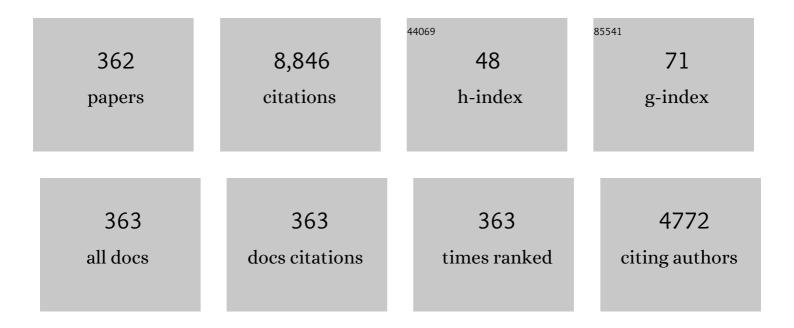
Pere Roca I Cabarrocas

List of Publications by Year in descending order

Source: https://exaly.com/author-pdf/8254189/publications.pdf Version: 2024-02-01



#	Article	IF	CITATIONS
1	A fully automated hotâ€wall multiplasmaâ€monochamber reactor for thin film deposition. Journal of Vacuum Science and Technology A: Vacuum, Surfaces and Films, 1991, 9, 2331-2341.	2.1	226
2	Plasma enhanced chemical vapor deposition of amorphous, polymorphous and microcrystalline silicon films. Journal of Non-Crystalline Solids, 2000, 266-269, 31-37.	3.1	184
3	Structure and hydrogen content of polymorphous silicon thin films studied by spectroscopic ellipsometry and nuclear measurements. Physical Review B, 2004, 69, .	3.2	159
4	Substrate selectivity in the formation of microcrystalline silicon: Mechanisms and technological consequences. Applied Physics Letters, 1995, 66, 3609-3611.	3.3	149
5	Influence of Cu as a catalyst on the properties of silicon nanowires synthesized by the vapour–solid–solid mechanism. Nanotechnology, 2007, 18, 305606.	2.6	144
6	Real-time spectroscopic ellipsometry study of the growth of amorphous and microcrystalline silicon thin films prepared by alternating silicon deposition and hydrogen plasma treatment. Physical Review B, 1995, 52, 5136-5143.	3.2	130
7	Growth and optoelectronic properties of polymorphous silicon thin films. Thin Solid Films, 2002, 403-404, 39-46.	1.8	124
8	Ion bombardment effects on microcrystalline silicon growth mechanisms and on the film properties. Journal of Applied Physics, 2003, 93, 1262-1273.	2.5	114
9	a-Si:H Deposition from SiH4and Si2H6rf-Discharges: Pressure and Temperature Dependence of Film Growth in Relation to α-γ Discharge Transition. Japanese Journal of Applied Physics, 1988, 27, 2041-2052.	1.5	110
10	Plasma-enhanced low temperature growth of silicon nanowires and hierarchical structures by using tin and indium catalysts. Nanotechnology, 2009, 20, 225604.	2.6	110
11	High efficiency and stable hydrogenated amorphous silicon radial junction solar cells built on VLS-grown silicon nanowires. Solar Energy Materials and Solar Cells, 2013, 118, 90-95.	6.2	107
12	Plasma texturing for silicon solar cells: From pyramids to inverted pyramids-like structures. Solar Energy Materials and Solar Cells, 2010, 94, 733-737.	6.2	99
13	Midgap density of states in hydrogenated polymorphous silicon. Journal of Applied Physics, 1999, 86, 946-950.	2.5	96
14	Contribution of ions to the growth of amorphous, polymorphous, and microcrystalline silicon thin films. Journal of Applied Physics, 2000, 88, 3674-3688.	2.5	93
15	Incorporation and redistribution of impurities into silicon nanowires during metal-particle-assisted growth. Nature Communications, 2014, 5, 4134.	12.8	91
16	Influence of the (111) twinning on the formation of diamond cubic/diamond hexagonal heterostructures in Cu-catalyzed Si nanowires. Journal of Applied Physics, 2008, 104, .	2.5	86
17	Insituinvestigation of the growth of rf glowâ€discharge deposited amorphous germanium and silicon films. Journal of Applied Physics, 1987, 61, 2501-2508.	2.5	84
18	Stable microcrystalline silicon thin-film transistors produced by the layer-by-layer technique. Journal of Applied Physics, 1999, 86, 7079-7082.	2.5	82

#	Article	IF	CITATIONS
19	In situ generation of indium catalysts to grow crystalline silicon nanowires at low temperature on ITO. Journal of Materials Chemistry, 2008, 18, 5187.	6.7	81
20	Ultrathin Epitaxial Silicon Solar Cells with Inverted Nanopyramid Arrays for Efficient Light Trapping. Nano Letters, 2016, 16, 5358-5364.	9.1	78
21	Bismuth-Catalyzed and Doped Silicon Nanowires for One-Pump-Down Fabrication of Radial Junction Solar Cells. Nano Letters, 2012, 12, 4153-4158.	9.1	76
22	Atomic structure of the nanocrystalline Si particles appearing in nanostructured Si thin films produced in low-temperature radiofrequency plasmas. Journal of Applied Physics, 2002, 92, 4684-4694.	2.5	74
23	Plasma production of nanocrystalline silicon particles and polymorphous silicon thin films for large-area electronic devices. Pure and Applied Chemistry, 2002, 74, 359-367.	1.9	74
24	A review on plasma-assisted VLS synthesis of silicon nanowires and radial junction solar cells. Journal Physics D: Applied Physics, 2014, 47, 393001.	2.8	73
25	Insituinvestigation of the optoelectronic properties of transparent conducting oxide/amorphous silicon interfaces. Applied Physics Letters, 1989, 54, 2088-2090.	3.3	72
26	Synthesis of silicon nanocrystals in silane plasmas for nanoelectronics and large area electronic devices. Journal Physics D: Applied Physics, 2007, 40, 2258-2266.	2.8	72
27	Polymorphous silicon thin films produced in dusty plasmas: application to solar cells. Plasma Physics and Controlled Fusion, 2004, 46, B235-B243.	2.1	71
28	Shedding light on the growth of amorphous, polymorphous, protocrystalline and microcrystalline silicon thin films. Thin Solid Films, 2001, 383, 161-164.	1.8	69
29	Observation of Incubation Times in the Nucleation of Silicon Nanowires Obtained by the Vapor-Liquid-Solid Method. Japanese Journal of Applied Physics, 2006, 45, L190-L193.	1.5	68
30	An In-Plane Solid-Liquid-Solid Growth Mode for Self-Avoiding Lateral Silicon Nanowires. Physical Review Letters, 2009, 102, 125501.	7.8	68
31	Gallium assisted plasma enhanced chemical vapor deposition of silicon nanowires. Nanotechnology, 2009, 20, 155602.	2.6	68
32	Determination of the conduction band offset between hydrogenated amorphous silicon and crystalline silicon from surface inversion layer conductance measurements. Applied Physics Letters, 2008, 92, 162101.	3.3	67
33	Role of mobile hydrogen in the amorphous silicon recrystallization. Applied Physics Letters, 1995, 66, 3146-3148.	3.3	62
34	Plasma enhanced chemical vapor deposition of silicon thin films for large area electronics. Current Opinion in Solid State and Materials Science, 2002, 6, 439-444.	11.5	62
35	In situcorrelation between the optical and electrical properties of thin intrinsic and n-type microcrystalline silicon films. Journal of Applied Physics, 1997, 81, 7282-7288.	2.5	61
36	Numerical modeling of capacitively coupled hydrogen plasmas: Effects of frequency and pressure. Journal of Applied Physics, 2003, 93, 3198-3206.	2.5	60

Pere Roca I Cabarrocas

#	Article	IF	CITATIONS
37	Effect of Wettability on the Agglomeration of Silicon Nanowire Arrays Fabricated by Metal-Assisted Chemical Etching. Langmuir, 2014, 30, 10290-10298.	3.5	60
38	Photonic nanostructures for advanced light trapping in thin crystalline silicon solar cells. Physica Status Solidi (A) Applications and Materials Science, 2015, 212, 140-155.	1.8	57
39	Absorbing photonic crystals for silicon thin-film solar cells: Design, fabrication and experimental investigation. Solar Energy Materials and Solar Cells, 2011, 95, S32-S38.	6.2	56
40	Very low densities of localized states at the Fermi level in hydrogenated polymorphous silicon from capacitance and space-charge-limited current measurements. Applied Physics Letters, 1999, 75, 3351-3353.	3.3	55
41	Low-temperature growth of thick intrinsic and ultrathin phosphorous or boron-doped microcrystalline silicon films: Optimum crystalline fractions for solar cell applications. Solar Energy Materials and Solar Cells, 2001, 69, 217-239.	6.2	55
42	Growth mechanism and dynamics of in-plane solid-liquid-solid silicon nanowires. Physical Review B, 2010, 81, .	3.2	54
43	In situ investigation of polymorphous silicon deposition. Journal of Non-Crystalline Solids, 2000, 266-269, 48-53.	3.1	50
44	Synthesis, morphology and compositional evolution of silicon nanowires directly grown on SnO2substrates. Nanotechnology, 2008, 19, 485605.	2.6	50
45	New features of the layerâ€byâ€layer deposition of microcrystalline silicon films revealed by spectroscopic ellipsometry and high resolution transmission electron microscopy. Applied Physics Letters, 1996, 69, 529-531.	3.3	49
46	Measurement of the in-depth stress profile in hydrogenated microcrystalline silicon thin films using Raman spectrometry. Journal of Applied Physics, 2001, 90, 3276-3279.	2.5	49
47	Growth study of indium-catalyzed silicon nanowires by plasma enhanced chemical vapor deposition. Applied Physics A: Materials Science and Processing, 2010, 100, 287-296.	2.3	49
48	Engineering island-chain silicon nanowires via a droplet mediated Plateau-Rayleigh transformation. Nature Communications, 2016, 7, 12836.	12.8	49
49	Hydrogen-effusion-induced structural changes and defects ina-Si:H films: Dependence upon the film microstructure. Physical Review B, 1996, 53, 3804-3812.	3.2	48
50	Effects of ion energy on the crystal size and hydrogen bonding in plasma-deposited nanocrystalline silicon thin films. Journal of Applied Physics, 2005, 97, 104334.	2.5	48
51	Some electronic and metastability properties of a new nanostructured material: Hydrogenated polymorphous silicon. The Philosophical Magazine: Physics of Condensed Matter B, Statistical Mechanics, Electronic, Optical and Magnetic Properties, 1999, 79, 1079-1095.	0.6	47
52	Soft landing of silicon nanocrystals in plasma enhanced chemical vapor deposition. Applied Physics Letters, 2006, 88, 203111.	3.3	47
53	Silicon nanowire solar cells grown by PECVD. Journal of Non-Crystalline Solids, 2012, 358, 2299-2302.	3.1	47
54	Optoelectronic properties of hydrogenated amorphous silicon films deposited under negative substrate bias. Journal of Applied Physics, 1991, 69, 2942-2950.	2.5	46

#	Article	IF	CITATIONS
55	Analysis and optimization of the performance of polymorphous silicon solar cells: Experimental characterization and computer modeling. Journal of Applied Physics, 2003, 94, 7305-7316.	2.5	46
56	Defect Formation in Ga-Catalyzed Silicon Nanowires. Crystal Growth and Design, 2010, 10, 1534-1543.	3.0	46
57	Nanopatterned front contact for broadband absorption in ultra-thin amorphous silicon solar cells. Applied Physics Letters, 2012, 101, 163901.	3.3	46
58	Dependence of the saturated lightâ€induced defect density on macroscopic properties of hydrogenated amorphous silicon. Applied Physics Letters, 1990, 57, 1440-1442.	3.3	45
59	New approaches for the production of nano-, micro-, and polycrystalline silicon thin films. Physica Status Solidi C: Current Topics in Solid State Physics, 2004, 1, 1115-1130.	0.8	44
60	Wetting Layer: The Key Player in Plasma-Assisted Silicon Nanowire Growth Mediated by Tin. Journal of Physical Chemistry C, 2013, 117, 17786-17790.	3.1	44
61	A comparative study of wet and dry texturing processes of c-Si wafers for the fabrication of solar cells. Solar Energy, 2014, 101, 182-191.	6.1	44
62	Understanding Light Harvesting in Radial Junction Amorphous Silicon Thin Film Solar Cells. Scientific Reports, 2015, 4, 4357.	3.3	44
63	Dangling-bond defect state creation in microcrystalline silicon thin-film transistors. Applied Physics Letters, 2000, 77, 750-752.	3.3	43
64	Initial nucleation and growth of in-plane solid-liquid-solid silicon nanowires catalyzed by indium. Physical Review B, 2009, 80, .	3.2	43
65	All-in-situ fabrication and characterization of silicon nanowires on TCO/glass substrates for photovoltaic application. Solar Energy Materials and Solar Cells, 2010, 94, 1855-1859.	6.2	43
66	Determination of the mobility gap of microcrystalline silicon and of the band discontinuities at the amorphous/microcrystalline silicon interface using in situ Kelvin probe technique. Applied Physics Letters, 1999, 74, 3218-3220.	3.3	42
67	Radial junction amorphous silicon solar cells on PECVD-grown silicon nanowires. Nanotechnology, 2012, 23, 194011.	2.6	42
68	Deterministic Line-Shape Programming of Silicon Nanowires for Extremely Stretchable Springs and Electronics. Nano Letters, 2017, 17, 7638-7646.	9.1	41
69	Investigation of coupling between chemistry and discharge dynamics in radio frequency hydrogen plasmas in the Torr regime. Journal Physics D: Applied Physics, 2004, 37, 1765-1773.	2.8	40
70	Hybrid solar cells based on thin-film silicon and P3HT. EPJ Applied Physics, 2006, 36, 231-234.	0.7	39
71	Core-shell structure and unique faceting of Sn-catalyzed silicon nanowires. Applied Physics Letters, 2010, 97, 023107.	3.3	39
72	Hydrogen-plasma etching of hydrogenated amorphous silicon: a study by a combination of spectroscopic ellipsometry and trap-limited diffusion model. Philosophical Magazine, 2004, 84, 595-609.	1.6	38

#	Article	IF	CITATIONS
73	Hydrogen diffusion and induced-crystallization in intrinsic and doped hydrogenated amorphous silicon films. Thin Solid Films, 2005, 487, 126-131.	1.8	38
74	Growth-in-place deployment of in-plane silicon nanowires. Applied Physics Letters, 2011, 99, .	3.3	38
75	Observation by infrared transmission spectroscopy and infrared ellipsometry of a new hydrogen bond during light-soaking of a-Si:H. The Philosophical Magazine: Physics of Condensed Matter B, Statistical Mechanics, Electronic, Optical and Magnetic Properties, 1995, 72, 363-372.	0.6	37
76	Determination of band offsets in a-Si:H/c-Si heterojunctions from capacitance–voltage measurements: Capabilities and limits. Thin Solid Films, 2007, 515, 7481-7485.	1.8	37
77	Guided growth of in-plane silicon nanowires. Applied Physics Letters, 2009, 95, .	3.3	37
78	Black Silicon formation using dry etching for solar cells applications. Materials Science and Engineering B: Solid-State Materials for Advanced Technology, 2012, 177, 1509-1513.	3.5	37
79	Snâ€catalyzed silicon nanowire solar cells with 4.9% efficiency grown on glass. Progress in Photovoltaics: Research and Applications, 2013, 21, 77-81.	8.1	37
80	Sol–Gel Route Toward Efficient and Robust Distributed Bragg Reflectors for Light Management Applications. Advanced Optical Materials, 2014, 2, 1105-1112.	7.3	36
81	Low temperature growth of highly crystallized silicon thin films using hydrogen and argon dilution. Journal of Non-Crystalline Solids, 1998, 227-230, 852-856.	3.1	35
82	Improvement of crystalline silicon surface passivation by hydrogen plasma treatment. Applied Physics Letters, 2004, 84, 1474-1476.	3.3	35
83	Irreversible light-induced degradation and stabilization of hydrogenated polymorphous silicon solar cells. Solar Energy Materials and Solar Cells, 2012, 105, 208-212.	6.2	35
84	New Approaches to Improve the Performance of Thin-Film Radial Junction Solar Cells Built Over Silicon Nanowire Arrays. IEEE Journal of Photovoltaics, 2015, 5, 40-45.	2.5	35
85	Silane versus silicon tetrafluoride in the growth of microcrystalline silicon films by standard radio frequency glow discharge. Thin Solid Films, 2007, 515, 7451-7454.	1.8	34
86	X-Ray diffraction and Raman spectroscopy for a better understanding of ZnO:Al growth process. EPJ Photovoltaics, 2011, 2, 25002.	1.6	34
87	Low temperature plasma deposition of silicon thin films: From amorphous to crystalline. Journal of Non-Crystalline Solids, 2012, 358, 2000-2003.	3.1	34
88	Inâ€Plane Selfâ€Turning and Twin Dynamics Renders Large Stretchability to Monoâ€Like Zigzag Silicon Nanowire Springs. Advanced Functional Materials, 2016, 26, 5352-5359.	14.9	34
89	Natural occurrence of the diamond hexagonal structure in silicon nanowires grown by a plasma-assisted vapour–liquid–solid method. Nanoscale, 2017, 9, 8113-8118.	5.6	34
90	Insitustudy of the thermal decomposition of B2H6by combining spectroscopic ellipsometry and Kelvin probe measurements. Journal of Applied Physics, 1989, 66, 3286-3292.	2.5	33

#	Article	IF	CITATIONS
91	Theoretical short-circuit current density for different geometries and organizations of silicon nanowires in solar cells. Solar Energy Materials and Solar Cells, 2013, 117, 645-651.	6.2	33
92	High performance transparent in-plane silicon nanowire Fin-TFTs via a robust nano-droplet-scanning crystallization dynamics. Nanoscale, 2017, 9, 10350-10357.	5.6	33
93	Plasma Deposition of Silicon Clusters: A Way to Produce Silicon Thin Films With Medium-Range Order ?. Materials Research Society Symposia Proceedings, 1998, 507, 855.	0.1	32
94	Quantification of the bond-angle dispersion by Raman spectroscopy and the strain energy of amorphous silicon. Journal of Applied Physics, 2008, 104, .	2.5	32
95	Criteria for improved open-circuit voltage in aâ€Si:H(N)â^•câ€Si(P) front heterojunction with intrinsic thin layer solar cells. Journal of Applied Physics, 2008, 103, 034506.	2.5	32
96	Thin crystalline silicon solar cells based on epitaxial films grown at 165°C by RF-PECVD. Solar Energy Materials and Solar Cells, 2011, 95, 2260-2263.	6.2	32
97	Microstructural, optical and electrical properties of annealed ZnO:Al thin films. Thin Solid Films, 2013, 531, 424-429.	1.8	32
98	Ultrathin PECVD epitaxial Si solar cells on glass via low-temperature transfer process. Progress in Photovoltaics: Research and Applications, 2016, 24, 1075-1084.	8.1	32
99	Core–Shell Heterojunction Solar Cells Based on Disordered Silicon Nanowire Arrays. Journal of Physical Chemistry C, 2016, 120, 2962-2972.	3.1	32
100	Deposition of intrinsic, phosphorusâ€doped, and boronâ€doped hydrogenated amorphous silicon films at 50 °C. Applied Physics Letters, 1994, 65, 1674-1676.	3.3	31
101	Large Area Deposition of Polymorphous Silicon by Plasma Enhanced Chemical Vapor Deposition at 27.12 MHz and 13.56 MHz. Japanese Journal of Applied Physics, 2003, 42, 4935-4942.	1.5	31
102	Stability and evolution of low-surface-tension metal catalyzed growth of silicon nanowires. Applied Physics Letters, 2011, 98, .	3.3	31
103	In-Plane Epitaxial Growth of Silicon Nanowires and Junction Formation on Si(100) Substrates. Nano Letters, 2014, 14, 6469-6474.	9.1	31
104	Effect of the Nanoparticles on the Structure and Crystallization of Amorphous Silicon Thin Films Produced by rf Glow Discharge. Journal of Materials Research, 1998, 13, 2476-2479.	2.6	30
105	Plasma-Assisted Growth of Silicon Nanowires by Sn Catalyst: Step-by-Step Observation. Nanoscale Research Letters, 2016, 11, 455.	5.7	29
106	Rational design of nanowire solar cells: from single nanowire to nanowire arrays. Nanotechnology, 2019, 30, 194002.	2.6	29
107	Hydrogen, microstructure and defect density in hydrogenated amorphous silicon. Journal De Physique, I, 1992, 2, 1979-1998.	1.2	28
108	Insitumeasurements of changes in the structure and in the excess charge arrier kinetics at the silicon surface during hydrogen and helium plasma exposure. Journal of Applied Physics, 1995, 78, 1438-1445.	2.5	28

#	Article	IF	CITATIONS
109	Dry fabrication process for heterojunction solar cells through in-situ plasma cleaning and passivation. Solar Energy Materials and Solar Cells, 2010, 94, 402-405.	6.2	28
110	Low temperature plasma enhanced CVD epitaxial growth of silicon on GaAs: a new paradigm for III-V/Si integration. Scientific Reports, 2016, 6, 25674.	3.3	28
111	Depositionâ€induced defect profiles in amorphous hydrogenated silicon. Applied Physics Letters, 1990, 56, 2448-2450.	3.3	27
112	Role of Si–H bonding ina‧i:H metastability. Journal of Applied Physics, 1996, 80, 97-102.	2.5	27
113	Critical issues in plasma deposition of microcrystalline silicon for thin film transistors. Solid-State Electronics, 2008, 52, 422-426.	1.4	27
114	Real-time measurement of the evolution of carrier mobility in thin-film semiconductors during growth. Applied Physics Letters, 1999, 74, 58-60.	3.3	26
115	Effects of the substrate temperature on the growth and properties of hydrogenated nanostructured silicon thin films. Journal Physics D: Applied Physics, 2001, 34, 690-699.	2.8	26
116	Properties of polymorphous silicon–germanium alloys deposited under high hydrogen dilution and at high pressure. Journal of Applied Physics, 2002, 92, 4959-4967.	2.5	26
117	Ultra-thin crystalline silicon films produced by plasma assisted epitaxial growth on silicon wafers and their transfer to foreign substrates. EPJ Photovoltaics, 2010, 1, 10301.	1.6	26
118	Optical characterization of hydrogenated silicon thin films using interference technique. Journal of Applied Physics, 2000, 88, 1907-1915.	2.5	25
119	Low temperature epitaxial growth of SiGe absorber for thin film heterojunction solar cells. Solar Energy Materials and Solar Cells, 2015, 134, 15-21.	6.2	25
120	Firmly standing three-dimensional radial junctions on soft aluminum foils enable extremely low cost flexible thin film solar cells with very high power-to-weight performance. Nano Energy, 2018, 53, 83-90.	16.0	25
121	Realization of heterostructures by pulsed laser induced epitaxy of C+ implanted pseudomorphic SiGe films and of a-SiGeC: H films deposited on Si(100). Journal of Crystal Growth, 1995, 157, 436-441.	1.5	24
122	Optimum doping level in a-Si:H and a-SiC:H materials. Journal of Applied Physics, 1998, 83, 830-836.	2.5	24
123	Optimization of plasma parameters for the production of silicon nano-crystals. New Journal of Physics, 2003, 5, 37-37.	2.9	24
124	Ultra-shallow junctions formed by quasi-epitaxial growth of boron and phosphorous-doped silicon films at 175 ðC by rf-PECVD. Thin Solid Films, 2010, 518, 2528-2530.	1.8	24
125	Strongly enhanced tunable photoluminescence in polymorphous silicon carbon thin films via excitation-transfer mechanism. Applied Physics Letters, 2010, 97, .	3.3	24
126	Substrate versus superstrate configuration for stable thin film silicon solar cells. Solar Energy Materials and Solar Cells, 2013, 119, 124-128.	6.2	24

#	Article	IF	CITATIONS
127	Optical properties and performance of pyramidal texture silicon heterojunction solar cells: <scp>K</scp> ey role of vertex angles. Progress in Photovoltaics: Research and Applications, 2018, 26, 369-376.	8.1	24
128	Insituinvestigation of the amorphous silicon/silicon nitride interfaces by spectroellipsometry. Journal of Applied Physics, 1991, 70, 2132-2135.	2.5	23
129	Microcrystalline Silicon Thin-Films Grown by Plasma Enhanced Chemical Vapour Deposition - Growth Mechanisms and Grain Size Control. Solid State Phenomena, 2003, 93, 257-268.	0.3	23
130	Contribution of plasma generated nanocrystals to the growth of microcrystalline silicon thin films. Journal of Non-Crystalline Solids, 2004, 338-340, 86-90.	3.1	23
131	Low temperature plasma synthesis of silicon nanocrystals: a strategy for high deposition rate and efficient polymorphous and microcrystalline solar cells. Plasma Physics and Controlled Fusion, 2008, 50, 124037.	2.1	23
132	Assessing individual radial junction solar cells over millions on VLS-grown silicon nanowires. Nanotechnology, 2013, 24, 275401.	2.6	23
133	Normal and anti Meyer–Neldel rule in conductivity of highly crystallized undoped microcrystalline silicon films. Journal of Non-Crystalline Solids, 2008, 354, 2263-2267.	3.1	22
134	Operating principles of in-plane silicon nanowires at simple step-edges. Nanoscale, 2015, 7, 5197-5202.	5.6	22
135	Transport mechanisms in hydrogenated microcrystalline silicon. Thin Solid Films, 2001, 383, 53-56.	1.8	21
136	No benefit from microcrystalline siliconNlayers in single junction amorphous silicon p-i-n solar cells. Journal of Applied Physics, 2003, 93, 170-174.	2.5	21
137	Luminescence of polymorphous silicon carbon alloys. Optical Materials, 2005, 27, 953-957.	3.6	21
138	Growth dynamics of hydrogenated silicon nanoparticles under realistic conditions of a plasma reactor. Computational Materials Science, 2006, 35, 216-222.	3.0	21
139	Experimental evidence for extended hydrogen diffusion in silicon thin films during light-soaking. Journal of Non-Crystalline Solids, 2006, 352, 1083-1086.	3.1	21
140	Calorimetry of dehydrogenation and dangling-bond recombination in several hydrogenated amorphous silicon materials. Physical Review B, 2006, 73, .	3.2	21
141	High interfacial conductivity at amorphous silicon/crystalline silicon heterojunctions. Journal of Non-Crystalline Solids, 2008, 354, 2641-2645.	3.1	21
142	Temperature dependence of the optical functions of amorphous silicon-based materials: application to in situ temperature measurements by spectroscopic ellipsometry. Thin Solid Films, 2004, 468, 298-302.	1.8	20
143	Large grain μc-Si:H films deposited at low temperature: Growth process and electronic properties. Journal of Non-Crystalline Solids, 2006, 352, 964-967.	3.1	20
144	Device grade hydrogenated polymorphous silicon deposited at high rates. Journal of Non-Crystalline Solids, 2008, 354, 2092-2095.	3.1	20

#	Article	IF	CITATIONS
145	Full potential of radial junction Si thin film solar cells with advanced junction materials and design. Applied Physics Letters, 2015, 107, .	3.3	20
146	Sunlight-thin nanophotonic monocrystalline silicon solar cells. Nano Futures, 2017, 1, 021001.	2.2	20
147	Ionâ€induced secondary electron emission in SiH4glow discharge, and temperature dependence of hydrogenated amorphous silicon deposition rate. Journal of Applied Physics, 1993, 73, 2578-2580.	2.5	19
148	Advances in the deposition of microcrystalline silicon at high rate by distributed electron cyclotron resonance. Thin Solid Films, 2008, 516, 6834-6838.	1.8	19
149	Long range effects of hydrogen during microcrystalline silicon growth. Thin Solid Films, 1997, 296, 11-14.	1.8	18
150	Growth mechanisms and structural properties of microcrystalline silicon films deposited by catalytic CVD. Thin Solid Films, 2001, 395, 178-183.	1.8	18
151	Experimental study and modeling of reverse-bias dark currents in PIN structures using amorphous and polymorphous silicon. Journal of Applied Physics, 2003, 94, 7317-7327.	2.5	18
152	The open-circuit voltage in microcrystalline silicon solar cells of different degrees of crystallinity. Thin Solid Films, 2008, 516, 6974-6978.	1.8	18
153	Bi-Sn alloy catalyst for simultaneous morphology and doping control of silicon nanowires in radial junction solar cells. Applied Physics Letters, 2015, 107, .	3.3	18
154	Heteroepitaxial Writing of Silicon-on-Sapphire Nanowires. Nano Letters, 2016, 16, 7317-7324.	9.1	18
155	Unravelling a simple method for the low temperature synthesis of silicon nanocrystals and monolithic nanocrystalline thin films. Scientific Reports, 2017, 7, 40553.	3.3	18
156	Growth of In-Plane Ge _{1–<i>x</i>} Sn _{<i>x</i>} Nanowires with 22 at. % Sn Using a Solid–Liquid–Solid Mechanism. Journal of Physical Chemistry C, 2018, 122, 26236-26242.	3.1	18
157	Highly flexible radial tandem junction thin film solar cells with excellent power-to-weight ratio. Nano Energy, 2021, 86, 106121.	16.0	18
158	Studies by photothermal deflection spectroscopy of defect formation in a-Si:H. The Philosophical Magazine: Physics of Condensed Matter B, Statistical Mechanics, Electronic, Optical and Magnetic Properties, 1991, 63, 143-150.	0.6	17
159	Experimental evidence for the annealing of surface defects inaâ€Si:H during deposition. Journal of Applied Physics, 1992, 72, 4727-4731.	2.5	17
160	Multilayered silicon/silicon nitride thin films deposited by plasma-CVD: Effects of crystallization. Scripta Materialia, 1995, 6, 843-846.	0.5	17
161	Plasma studies under polymorphous silicon deposition conditions. Thin Solid Films, 2003, 427, 236-240.	1.8	17
162	Crystallization kinetics of hydrogenated amorphous silicon thick films grown by plasma-enhanced chemical vapour deposition. Applied Surface Science, 2004, 238, 165-168.	6.1	17

#	Article	IF	CITATIONS
163	Study of radial growth rate and size control of silicon nanocrystals in square-wave-modulated silane plasmas. Applied Physics Letters, 2007, 91, 111501.	3.3	17
164	Study of the effects of different fractions of large grains of μc-Si:H:F films on the infrared absorption on thin film solar cells. Solar Energy Materials and Solar Cells, 2012, 100, 16-20.	6.2	17
165	Fine-tuning of the interface in high-quality epitaxial silicon films deposited by plasma-enhanced chemical vapor deposition at 200 °C. Journal of Materials Research, 2013, 28, 1626-1632.	2.6	17
166	Understanding the amorphous-to-microcrystalline silicon transition in SiF4/H2/Ar gas mixtures. Journal of Chemical Physics, 2014, 140, 234706.	3.0	17
167	Cross-Sectional Investigations on Epitaxial Silicon Solar Cells by Kelvin and Conducting Probe Atomic Force Microscopy: Effect of Illumination. Nanoscale Research Letters, 2016, 11, 55.	5.7	17
168	Low-Temperature Plasma-Assisted Growth of Core–Shell GeSn Nanowires with 30% Sn. Journal of Physical Chemistry C, 2020, 124, 1220-1226.	3.1	17
169	Time resolved microwave conductivity measurements for the characterization of transport properties in thin film micro-crystalline silicon. Thin Solid Films, 1997, 296, 94-97.	1.8	16
170	Role of hydrogen diffusion on the growth of polymorphous and microcrystalline silicon thin films. EPJ Applied Physics, 2006, 35, 165-172.	0.7	16
171	Why does the open-circuit voltage in a micro-crystalline silicon PIN solar cell decrease with increasing crystalline volume fraction?. Journal of Non-Crystalline Solids, 2008, 354, 2455-2459.	3.1	16
172	Ion Energy Threshold in Low-Temperature Silicon Epitaxy for Thin-Film Crystalline Photovoltaics. IEEE Journal of Photovoltaics, 2014, 4, 1361-1367.	2.5	16
173	Structural properties of relaxed thin film germanium layers grown by low temperature RF-PECVD epitaxy on Si and Ge (100) substrates. AIP Advances, 2014, 4, .	1.3	16
174	Influence of deposition rate on the structural properties of plasma-enhanced CVD epitaxial silicon. Scientific Reports, 2017, 7, 43968.	3.3	16
175	Nanodroplet Hydrodynamic Transformation of Uniform Amorphous Bilayer into Highly Modulated Ge/Si Island-Chains. Nano Letters, 2018, 18, 6931-6940.	9.1	16
176	Analytical compensation of stray capacitance effect in Kelvin probe measurements. Review of Scientific Instruments, 1995, 66, 5272-5276.	1.3	15
177	Structural properties depicted by optical measurements in hydrogenated polymorphous silicon. Journal of Physics Condensed Matter, 1999, 11, 8749-8757.	1.8	15
178	Very low surface recombination velocity of crystalline silicon passivated by phosphorusâ€doped <i>aâ€6ic_xN_y:H(n)</i> alloys. Progress in Photovoltaics: Research and Applications, 2008, 16, 123-127.	8.1	15
179	Directional growth of Ge on GaAs at 175°C using plasma-generated nanocrystals. Applied Physics Letters, 2008, 92, 103108.	3.3	15
180	How tilting and cavity-mode-resonant absorption contribute to light harvesting in 3D radial junction solar cells. Optics Express, 2015, 23, A1288.	3.4	15

#	Article	IF	CITATIONS
181	Effect of deposition temperature on polymorphous silicon thin films by PECVD: Role of hydrogen. Materials Science in Semiconductor Processing, 2016, 41, 390-397.	4.0	15
182	Biomimetic Radial Tandem Junction Photodetector with Natural RGB Color Discrimination Capability. Advanced Optical Materials, 2017, 5, 1700390.	7.3	15
183	Microcrystalline silicon: An emerging material for stable thin-film transistors. Journal of the Society for Information Display, 2004, 12, 3.	2.1	14
184	About the efficiency limits of heterojunction solar cells. Journal of Non-Crystalline Solids, 2006, 352, 1928-1932.	3.1	14
185	Strong orange/red electroluminescence from hydrogenated polymorphous silicon carbon light-emitting devices. Applied Physics Letters, 2008, 92, .	3.3	14
186	Electronic and structural properties of the amorphous/crystalline silicon interface. Thin Solid Films, 2009, 517, 6386-6391.	1.8	14
187	Low Temperature Plasma Synthesis of Nanocrystals and their Application to the Growth of Crystalline Silicon and Germanium Thin Films. Materials Research Society Symposia Proceedings, 2012, 1426, 319-329.	0.1	14
188	Large Area Radial Junction Silicon Nanowire Solar Mini-Modules. Scientific Reports, 2018, 8, 1651.	3.3	14
189	Germanium quantum dot infrared photodetectors addressed by self-aligned silicon nanowire electrodes. Nanotechnology, 2020, 31, 145602.	2.6	14
190	Polymorphous Silicon Films Deposited at 27.12 MHz. Chemical Vapor Deposition, 2003, 9, 333-337.	1.3	13
191	Effect of deposition conditions and dielectric plasma treatments on the electrical properties of microcrystalline silicon TFTs. Thin Solid Films, 2003, 427, 67-70.	1.8	13
192	Structural determination of nanocrystalline Si films using ellipsometry and Raman spectroscopy. Thin Solid Films, 2008, 516, 6863-6868.	1.8	13
193	Interpretation of the hydrogen evolution during deposition of microcrystalline silicon by chemical transport. Thin Solid Films, 2009, 517, 6225-6229.	1.8	13
194	Light induced electrical and macroscopic changes in hydrogenated polymorphous silicon solar cells. EPJ Photovoltaics, 2012, 3, 30301.	1.6	13
195	Advanced radial junction thin film photovoltaics and detectors built on standing silicon nanowires. Nanotechnology, 2019, 30, 302001.	2.6	13
196	Study by real time ellipsometry of the growth of amorphous and microcrystalline silicon thin films combining glow discharge decomposition and UV light irradiation. Thin Solid Films, 1993, 233, 281-285.	1.8	12
197	Over-coordination and order in hydrogenated nanostructured silicon thin films: their influence on strain and electronic properties. Journal of Physics Condensed Matter, 2005, 17, 1279-1288.	1.8	12
198	Progress in a-Si:H/c-Si heterojunction emitters obtained by Hot-Wire CVD at 200°C. Thin Solid Films, 2008, 516, 761-764.	1.8	12

#	Article	IF	CITATIONS
199	Epitaxial growth of silicon and germanium on (100)-oriented crystalline substrates by RF PECVD at 175 °C. EPJ Photovoltaics, 2012, 3, 30303.	1.6	12
200	Amorphous silicon diamond based heterojunctions with high rectification ratio. Journal of Non-Crystalline Solids, 2012, 358, 2110-2113.	3.1	12
201	Towards 12% stabilised efficiency in single junction polymorphous silicon solar cells: experimental developments and model predictions. EPJ Photovoltaics, 2016, 7, 70302.	1.6	12
202	Light-induced defect creation in hydrogenated polymorphous silicon. Materials Science and Engineering B: Solid-State Materials for Advanced Technology, 2005, 121, 34-41.	3.5	11
203	Influence of deposition parameters and post-deposition plasma treatments on the photoluminescence of polymorphous silicon carbon alloys. Journal of Non-Crystalline Solids, 2006, 352, 1357-1360.	3.1	11
204	Transition from thin gold layers to nanoâ€islands on TCO for catalyzing the growth of oneâ€dimensional nanostructures. Physica Status Solidi (A) Applications and Materials Science, 2008, 205, 1429-1434.	1.8	11
205	Microscopic measurements of variations in local (photo)electronic properties in nanostructured solar cells. Solar Energy Materials and Solar Cells, 2013, 119, 228-234.	6.2	11
206	Meandering growth of in-plane silicon nanowire springs. Applied Physics Letters, 2019, 114, .	3.3	11
207	Study of pm-SiGe:H thin films for p–i–n devices and tandem solar cells. Thin Solid Films, 2003, 427, 247-251.	1.8	10
208	Study of anomalous behavior of steady state photoconductivity in highly crystallized undoped microcrystalline Si films. Journal of Non-Crystalline Solids, 2006, 352, 1172-1175.	3.1	10
209	Influence of process steps on the performance of microcrystalline silicon thin film transistors. Thin Solid Films, 2007, 515, 7662-7666.	1.8	10
210	Role of microstructure in electronic transport behavior of highly crystallized undoped microcrystalline Si Films. Thin Solid Films, 2007, 515, 7469-7474.	1.8	10
211	Reliable Characterization of Microcrystalline Silicon Films for Thin Film Transistor Applications. Japanese Journal of Applied Physics, 2008, 47, 7308-7310.	1.5	10
212	Molecular hydrogen diffusion in nanostructured amorphous silicon thin films. Physical Review B, 2009, 80, .	3.2	10
213	Relaxation and derelaxation of pure and hydrogenated amorphous silicon during thermal annealing experiments. Applied Physics Letters, 2010, 97, 031918.	3.3	10
214	Hydrogen related crystallization in intrinsic hydrogenated amorphous silicon films prepared by reactive radiofrequency magnetron sputtering at low temperature. Thin Solid Films, 2012, 522, 186-192.	1.8	10
215	Doped semiconductor nanocrystal junctions. Journal of Applied Physics, 2013, 114, .	2.5	10
216	Deposition of microcrystalline silicon in electron-cyclotron resonance discharge (24GHz) plasma from silicon tetrafluoride precursor. Thin Solid Films, 2014, 562, 114-117.	1.8	10

#	Article	IF	CITATIONS
217	Optimization and optical characterization of vertical nanowire arrays for core-shell structure solar cells. Solar Energy Materials and Solar Cells, 2017, 159, 640-648.	6.2	10
218	In-situ Mueller matrix ellipsometry of silicon nanowires grown by plasma-enhanced vapor-liquid-solid method for radial junction solar cells. Applied Surface Science, 2017, 421, 667-673.	6.1	10
219	Toward Efficient Radial Junction Silicon Nanowireâ€Based Solar Miniâ€Modules. Physica Status Solidi - Rapid Research Letters, 2019, 13, 1800402.	2.4	10
220	Systematic study of light-induced effects in hydrogenated amorphous silicon. Physical Review B, 1992, 45, 13314-13322.	3.2	9
221	Acoustically induced optical second harmonic generation in hydrogenated amorphous silicon films. Journal Physics D: Applied Physics, 2003, 36, 713-718.	2.8	9
222	Device quality a-Si:H deposited from electron cyclotron resonance at very high deposition rates. Journal of Non-Crystalline Solids, 2006, 352, 1913-1916.	3.1	9
223	Threshold voltage shift under electrical stress in amorphous, polymorphous, and microcrystalline silicon bottom gate thinâ€film transistors. Physica Status Solidi (A) Applications and Materials Science, 2010, 207, 1245-1248.	1.8	9
224	Factors limiting the open-circuit voltage in microcrystalline silicon solar cells. EPJ Photovoltaics, 2011, 2, 20101.	1.6	9
225	High quality boron-doped epitaxial layers grown at 200°C from SiF4/H2/Ar gas mixtures for emitter formation in crystalline silicon solar cells. AIP Advances, 2017, 7, .	1.3	9
226	Structural study of NiOx thin films fabricated by radio frequency sputtering at low temperature. Thin Solid Films, 2018, 646, 209-215.	1.8	9
227	Liquid-Assisted Vapor–Solid–Solid Silicon Nanowire Growth Mechanism Revealed by <i>In Situ</i> TEM When Using Cu–Sn Bimetallic Catalysts. Journal of Physical Chemistry C, 2021, 125, 19773-19779.	3.1	9
228	Polymorphous silicon deposited in large area reactor at 13 and 27 MHz. Thin Solid Films, 2003, 427, 6-10.	1.8	8
229	Plasma diagnostics in silane–methane–hydrogen plasmas under pm-Si1â^'xCx:H deposition conditions: Correlation with film properties. Journal of Non-Crystalline Solids, 2006, 352, 959-963.	3.1	8
230	Microstructure and surface roughness study of highly crystallized μc-Si:H Films. Thin Solid Films, 2007, 515, 7619-7624.	1.8	8
231	New method for interface characterization in heterojunction solar cells based on diffusion capacitance measurements. Thin Solid Films, 2008, 516, 6786-6790.	1.8	8
232	Negative corona discharge: application to nanoparticle detection in rf reactors. Plasma Sources Science and Technology, 2009, 18, 015005.	3.1	8
233	Morphology control and growth dynamics of in-plane solid–liquid–solid silicon nanowires. Physica E: Low-Dimensional Systems and Nanostructures, 2012, 44, 1045-1049.	2.7	8
234	Hybrid System and Environmental Evaluation Case House in South of Algeria. Energy Procedia, 2013, 36, 1328-1338.	1.8	8

#	Article	IF	CITATIONS
235	Feasibility of using thin crystalline silicon films epitaxially grown at 165 °C in solar cells: A computer simulation study. EPJ Photovoltaics, 2013, 4, 45103.	1.6	8
236	Performance Analysis of AlxGa1-xAs/epi-Si(Ge) Tandem Solar Cells: A Simulation Study. Energy Procedia, 2015, 84, 41-46.	1.8	8
237	Atomic characterization of Au clusters in vapor-liquid-solid grown silicon nanowires. Journal of Applied Physics, 2015, 118, 104301.	2.5	8
238	Boosting light emission from Si-based thin film over Si and SiO_2 nanowires architecture. Optics Express, 2015, 23, 5388.	3.4	8
239	Influence of anodic bonding on the surface passivation quality of crystalline silicon. Solar Energy Materials and Solar Cells, 2016, 157, 154-160.	6.2	8
240	Nanophotonics-based low-temperature PECVD epitaxial crystalline silicon solar cells. Journal Physics D: Applied Physics, 2016, 49, 125603.	2.8	8
241	Plasma-enhanced chemical vapor deposition epitaxy of Si on GaAs for tunnel junction applications in tandem solar cells. Journal of Photonics for Energy, 2017, 7, 022504.	1.3	8
242	Growth of Tetragonal Si via Plasma-Enhanced Epitaxy. Crystal Growth and Design, 2017, 17, 4265-4269.	3.0	8
243	Light-induced effects on the optical absorption of a-Si:H. Journal of Non-Crystalline Solids, 1988, 104, 59-61.	3.1	7
244	Realâ€ŧime spectroellipsometry investigation of the interaction of silane with a Pd thin film: Formation of palladium silicides. Journal of Applied Physics, 1993, 74, 2535-2542.	2.5	7
245	What makes a thin films semiconductor suitable for solar cells applications?. Thin Solid Films, 2003, 427, 241-246.	1.8	7
246	Study of GeYSi1â^'Y:H films deposited by low frequency plasma. Thin Solid Films, 2007, 515, 7603-7606.	1.8	7
247	Numerical modeling of steady state photoconductivity process in highly crystallized undoped μc-Si:H films. Thin Solid Films, 2007, 515, 7576-7580.	1.8	7
248	Negative corona in silane–argon–hydrogen mixtures at low pressures. Journal Physics D: Applied Physics, 2008, 41, 165203.	2.8	7
249	Probing dusty-plasma/surface interactions with a heat flux microsensor. Applied Physics Letters, 2012, 100, .	3.3	7
250	Photoluminescence spectrum from heterojunction with intrinsic thin layer solar cells: An efficient tool for estimating wafer surface defects. Journal of Non-Crystalline Solids, 2012, 358, 2241-2244.	3.1	7
251	In-situ spectroscopic ellipsometry of microcrystalline silicon deposited by plasma-enhanced chemical vapor deposition on flexible Fe–Ni alloy substrate for photovoltaic applications. Thin Solid Films, 2014, 571, 749-755.	1.8	7
252	Substrate and p-layer effects on polymorphous silicon solar cells. EPJ Photovoltaics, 2014, 5, 55206.	1.6	7

#	Article	IF	CITATIONS
253	Hydrogen content, transport properties and light degradation of a-Si:H films containing artificially generated interfaces. Solar Energy Materials and Solar Cells, 1988, 17, 1-16.	0.4	6
254	Thermal quenching and relaxation in doped hydrogenated amorphous silicon deposited by plasmaâ€enhanced chemical vapor deposition from Heâ€diluted silane. Applied Physics Letters, 1993, 62, 594-596.	3.3	6
255	Substrate temperature effect on the stability of hydrogenated amorphous silicon films deposited at high rates. Journal of Applied Physics, 1995, 78, 317-320.	2.5	6
256	Role of Initial Vibrational and Rotational Reactant Excitation for the Reaction Dynamics of H2(ν0,J0) with Si+(2P). Journal of Physical Chemistry A, 2004, 108, 1818-1825.	2.5	6
257	Dispersive processes of light-induced defect creation in hydrogenated amorphous silicon. Solid State Communications, 2007, 142, 232-236.	1.9	6
258	Effect of substrate on hydrogen in and out diffusion from a-Si:H thin films. Journal of Materials Science: Materials in Electronics, 2007, 18, 1051-1056.	2.2	6
259	Distributed electron cyclotron resonance plasma: A technology for large area deposition of device-quality a-Si:H at very high rate. Thin Solid Films, 2008, 516, 6853-6857.	1.8	6
260	Electronic properties of embedded graphene: doped amorphous silicon/CVD graphene heterostructures. Journal of Physics Condensed Matter, 2016, 28, 404001.	1.8	6
261	Nanostructured back reflectors produced using polystyrene assisted lithography for enhanced light trapping in silicon thin film solar cells. Solar Energy, 2018, 167, 108-115.	6.1	6
262	Contactless electronic transport analysis of microcrystalline silicon. Thin Solid Films, 1999, 337, 63-66.	1.8	5
263	Photoinduced effects in RF and VHF a-Si:H films deposited with different ion bombardment. Thin Solid Films, 2001, 383, 178-180.	1.8	5
264	Thermally Induced Structural Transformations on Polymorphous Silicon. Journal of Materials Research, 2005, 20, 2562-2567.	2.6	5
265	Polymorphous silicon thin films deposited at high rate: Transport properties and density of states. Thin Solid Films, 2008, 516, 6888-6891.	1.8	5
266	Comparison of photoluminescence and capacitance spectroscopies as efficient tools for interface characterisation of heterojunction solar cells. Journal of Non-Crystalline Solids, 2008, 354, 2416-2420.	3.1	5
267	The kinetics of the light-induced defect creation in hydrogenated amorphous silicon – Stretched exponential relaxation. Journal of Non-Crystalline Solids, 2008, 354, 2131-2134.	3.1	5
268	Detailed study of surface and interface properties of μc-Si films. Journal of Non-Crystalline Solids, 2008, 354, 2218-2222.	3.1	5
269	Characterization of amorphous and nanostructured Si films by differential scanning calorimetry. Thin Solid Films, 2009, 517, 6239-6242.	1.8	5
270	Geometrical optimization and electrical performance comparison of thin-film tandem structures based on pm-Si:H andl1¼c-Si:H using computer simulation. EPJ Photovoltaics, 2011, 2, 20301.	1.6	5

#	Article	IF	CITATIONS
271	Mechanisms of Threshold Voltage Shift in Polymorphous and Microcrystalline Silicon Bottom Gate Thin-Film Transistors. Journal of Display Technology, 2012, 8, 23-26.	1.2	5
272	Influence of sputtering conditions on the optical and electrical properties of laser-annealed and wet-etched room temperature sputtered ZnO:Al thin films. Thin Solid Films, 2014, 555, 13-17.	1.8	5
273	Insights into gold-catalyzed plasma-assisted CVD growth of silicon nanowires. Applied Physics Letters, 2016, 109, .	3.3	5
274	Excellent Surface Passivation and Light Absorption in Crystalline Si via Low-Temperature Si Nanowire Growth. IEEE Journal of Photovoltaics, 2016, 6, 823-829.	2.5	5
275	Use of hexamethyldisiloxane for p-type microcrystalline silicon oxycarbide layers. EPJ Photovoltaics, 2016, 7, 70301.	1.6	5
276	On the Mechanism of In Nanoparticle Formation by Exposing ITO Thin Films to Hydrogen Plasmas. Langmuir, 2017, 33, 12114-12119.	3.5	5
277	Low temperature epitaxial growth of boron-doped silicon thin films. AIP Conference Proceedings, 2018, , .	0.4	5
278	Controlling solid–liquid–solid GeSn nanowire growth modes by changing deposition sequences of a-Ge:H layer and SnO ₂ nanoparticles. Nanotechnology, 2021, 32, 345602.	2.6	5
279	Impact of PECVD-prepared interfacial Si and SiGe layers on epitaxial Si films grown by PECVD (200°C) and APCVD (1130°C). Applied Surface Science, 2021, 546, 149056.	6.1	5
280	Detection of stable positive fixed charges in AlOx activated during annealing with in situ modulated PhotoLuminescence. Solar Energy Materials and Solar Cells, 2021, 230, 111172.	6.2	5
281	Insitumicrowave reflectivity measurements of the changes in surface recombination of crystalline silicon induced by the exposure to silane, silane/helium, and helium plasmas. Applied Physics Letters, 1994, 65, 1260-1262.	3.3	4
282	Bulk and surface structural properties of Si1â^'xâ^'yGexCy layers processed on Si(001) by pulsed laser induced epitaxy. Applied Surface Science, 1996, 102, 28-32.	6.1	4
283	Deposition parameters and surface topography of a-Si:H thin films obtained by the RF glow discharge process. Materials Science and Engineering B: Solid-State Materials for Advanced Technology, 1996, 42, 105-109.	3.5	4
284	Plasma deposition of carbon films at room temperature from C2H2–Ar mixtures: anodic vs. cathodic films. Thin Solid Films, 2001, 383, 216-219.	1.8	4
285	Effect of thermal coupling on the electronic properties of hydrogenated amorphous silicon thin films deposited by electron cyclotron resonance. Thin Solid Films, 2007, 515, 7650-7653.	1.8	4
286	Plasmas for texturing, cleaning, and deposition: towards a one pump down process for heterojunction solar cells. Physica Status Solidi C: Current Topics in Solid State Physics, 2010, 7, NA-NA.	0.8	4
287	High deposition rate hydrogenated polymorphous silicon characterized by different capacitance techniques. Thin Solid Films, 2011, 519, 5364-5370.	1.8	4
288	Effect of annealing on silicon heterojunction solar cells with textured ZnO:Al as transparent conductive oxide. EPJ Photovoltaics, 2012, 3, 35002.	1.6	4

#	Article	IF	CITATIONS
289	Influence of the fabrication conditions of polymorphous silicon films on their structural, electrical and optical properties. Semiconductors, 2013, 47, 1271-1274.	0.5	4
290	Raman spectra of amorphous isotope-enriched 74Ge with low-strained Ge nanocrystals. Thin Solid Films, 2014, 552, 46-49.	1.8	4
291	Nanoscale Investigation of Carrier Lifetime on the Cross Section of Epitaxial Silicon Solar Cells Using Kelvin Probe Force Microscopy. IEEE Journal of Photovoltaics, 2016, 6, 1576-1580.	2.5	4
292	Current-induced and light-induced macroscopic changes in thin film solar cells: Device degradation mechanism. Solar Energy, 2017, 143, 86-92.	6.1	4
293	Effect of Pressure and Flow Rates on Polymorphous Siliconâ€Germanium (pmâ€Si _x Ge _{1â~x} :H) Thin Films for Infrared Detection Applications. Physica Status Solidi (A) Applications and Materials Science, 2018, 215, 1700735.	1.8	4
294	Powder free PECVD epitaxial silicon by plasma pulsing or increasing the growth temperature. Journal Physics D: Applied Physics, 2018, 51, 235203.	2.8	4
295	Impact of charged species transport coefficients on self-bias voltage in an electrically asymmetric RF discharge. Plasma Sources Science and Technology, 2019, 28, 055003.	3.1	4
296	Interfacial hydrogen incorporation in epitaxial silicon for layer transfer. Applied Surface Science, 2020, 518, 146057.	6.1	4
297	Role of H3 + ions in deposition of silicon thin films from SiH4/H2 discharges: modeling and experiments. Plasma Sources Science and Technology, 2021, 30, 075024.	3.1	4
298	High Density of Quantum-Sized Silicon Nanowires with Different Polytypes Grown with Bimetallic Catalysts. ACS Omega, 2021, 6, 26381-26390.	3.5	4
299	In situ observation of droplet nanofluidics for yielding low-dimensional nanomaterials. Applied Surface Science, 2022, 573, 151510.	6.1	4
300	Precise morphology control of in-plane silicon nanowires via a simple plasma pre-treatment. Applied Surface Science, 2022, 593, 153435.	6.1	4
301	Effect of light soaking and annealing on the stability of hydrogenated amorphous silicon films deposited using pure and highly helium diluted silane. Solid State Communications, 2002, 122, 259-264.	1.9	3
302	DTRMC, a probe of transverse transport in microcrystalline silicon. Thin Solid Films, 2003, 427, 335-339.	1.8	3
303	Anomalous crystallization of hydrogenated amorphous silicon during fast heating ramps. Journal of Materials Research, 2005, 20, 277-281.	2.6	3
304	Influence of deposition parameters on hole mobility in polymorphous silicon. Thin Solid Films, 2007, 515, 7504-7507.	1.8	3
305	Optimization of electroluminescent diodes based on pm-SiC:H deposited at low temperature. Materials Science and Engineering B: Solid-State Materials for Advanced Technology, 2008, 147, 245-248.	3.5	3
306	Deleterious electrostatic interaction in silicon passivation stack between thin ALD Al2O3 and its a-SiNX:H capping layer: numerical and experimental evidences. Energy Procedia, 2017, 124, 91-98.	1.8	3

#	Article	IF	CITATIONS
307	Tin dioxide nanoparticles as catalyst precursors for plasma-assisted vapor–liquid–solid growth of silicon nanowires with well-controlled density. Nanotechnology, 2018, 29, 435301.	2.6	3
308	Influence of p- and n-type doping gases on nanoparticle formation in SiH4/H2 radiofrequency plasma discharges used for polymorphous silicon thin film deposition. Journal of Applied Physics, 2019, 125, 163307.	2.5	3
309	Annealing of Boron-Doped Hydrogenated Crystalline Silicon Grown at Low Temperature by PECVD. Materials, 2019, 12, 3795.	2.9	3
310	Effect of strain on the dark current-voltage characteristic of silicon heterojunction solar cells. Solar Energy, 2020, 196, 457-461.	6.1	3
311	Transmission electron microscopy characterization of low temperature boron doped silicon epitaxial films. CrystEngComm, 2020, 22, 5464-5472.	2.6	3
312	Hydrogen Plasma-Assisted Growth of Gold Nanowires. Crystal Growth and Design, 2020, 20, 4185-4192.	3.0	3
313	Room temperature growth of silica nanowires on top of ultrathin Si nanowires synthesized with Sn u bimetallic seeds. Physica Status Solidi (A) Applications and Materials Science, 2021, 218, 2100409.	1.8	3
314	Ultrathin Ge epilayers on Si produced by low-temperature PECVD acting as virtual substrates for III-V / c-Si tandem solar cells. Solar Energy Materials and Solar Cells, 2022, 236, 111535.	6.2	3
315	Non-linear optical diagnostic of a-Si:H thin films deposited by RF-glow discharge. Physica E: Low-Dimensional Systems and Nanostructures, 2006, 31, 132-135.	2.7	2
316	Structural properties of microcrystalline Si films prepared by hot-wire/catalytic chemical vapor deposition under conditions close to the transition from amorphous to microcrystalline growth. Thin Solid Films, 2011, 519, 4502-4505.	1.8	2
317	Characterization of defects in hydrogenated amorphous silicon deposited on different substrates by capacitance techniques. Thin Solid Films, 2011, 519, 5473-5480.	1.8	2
318	Measurement of the specific heat and determination of the thermodynamic functions of relaxed amorphous silicon. Journal of Applied Physics, 2013, 113, .	2.5	2
319	Polarized Raman spectroscopy analysis of SiHX bonds in nanocrystalline silicon thin films. Thin Solid Films, 2013, 537, 145-148.	1.8	2
320	Plasma-Texturing Processes and a-Si:H Surface Passivation on c-Si Wafers for Photovoltaic Applications. Journal of Solar Energy Engineering, Transactions of the ASME, 2015, 137, .	1.8	2
321	Effect of light-soaking on the hydrogen effusion mechanisms inÂpolymorphous silicon thin film structures. Materials Chemistry and Physics, 2015, 163, 311-316.	4.0	2
322	Hybrid kinetic/fluid modeling of silicon nanoparticles dynamics in silane plasma discharges. AIP Conference Proceedings, 2016, , .	0.4	2
323	Robustness up to 400°C of the passivation of c-Si by p-type a-Si:H thanks to ion implantation. AIP Advances, 2016, 6, 125107.	1.3	2
324	Three-dimensional atomic mapping of hydrogenated polymorphous silicon solar cells. Applied Physics Letters, 2016, 108, 253110.	3.3	2

#	Article	IF	CITATIONS
325	Effect of substrate temperature on the plasma texturing process of câ€6i wafers for black silicon solar cells. Physica Status Solidi (A) Applications and Materials Science, 2016, 213, 1937-1941.	1.8	2
326	A Solar Cell Architecture for Enhancing Performance While Reducing Absorber Thickness and Back Contact Requirements. IEEE Journal of Photovoltaics, 2017, 7, 974-979.	2.5	2
327	Comments on "Nanoscale Investigation of Carrier Lifetime on the Cross Section of Epitaxial Silicon Solar Cells Using Kelvin Probe Force Microscopy― IEEE Journal of Photovoltaics, 2018, 8, 661-663.	2.5	2
328	Influence of N-type μc-SiOx:H intermediate reflector and top cell material properties on the electrical performance of "micromorph―tandem solar cells. AIP Advances, 2018, 8, 015115.	1.3	2
329	In situ spectroscopic ellipsometry study of low-temperature epitaxial silicon growth. Photonics and Nanostructures - Fundamentals and Applications, 2018, 30, 73-77.	2.0	2
330	Assessment of High Sn Incorporation in Ge NanoWires Synthesized via In Plane Solid-Liquid-Solid Mechanism by In-Situ TEM. Microscopy and Microanalysis, 2018, 24, 306-307.	0.4	2
331	Impact of PECVD μc-Si:H deposition on tunnel oxide for passivating contacts. EPJ Photovoltaics, 2020, 11, 3.	1.6	2
332	Heteroepitaxial growth of silicon on GaAs via low-temperature plasma-enhanced chemical vapor deposition. , 2019, , .		2
333	Polymorphous Silicon: A Promising Material for Thin-Film Transistors for Low-Cost and High-Performance Active-Matrix OLED Displays. IEICE Transactions on Electronics, 2010, E93-C, 1490-1494.	0.6	2
334	Comparative Study on the Quality of Microcrystalline and Epitaxial Silicon Films Produced by PECVD Using Identical SiF4 Based Process Conditions. Materials, 2021, 14, 6947.	2.9	2
335	Rational Control of GeSn Nanowires. Physica Status Solidi - Rapid Research Letters, 0, , 2100554.	2.4	2
336	Investigation of Sn-containing precursors for in-plane GeSn nanowire growth. Journal of Alloys and Compounds, 2022, 899, 163273.	5.5	2
337	Visualizing the effects of plasma-generated H atoms <i>in situ</i> in a transmission electron microscope. EPJ Applied Physics, 2022, 97, 7.	0.7	2
338	New buffer concept inherent to pulsed laser induced epitaxy. Applied Physics Letters, 1998, 72, 2292-2294.	3.3	1
339	Effect of Dopants on the Dynamic of Powder Formation and the Properties of Polymorphous Silicon Thin Films. Materials Science Forum, 2004, 455-456, 536-539.	0.3	1
340	Influence of the deposition temperature on the performance of microcrystalline silicon thin film transistors. Solid-State Electronics, 2008, 52, 432-435.	1.4	1
341	Model calculation of phototransport properties of minority carriers of fully crystalline undoped µc-Si:H. Thin Solid Films, 2009, 517, 6248-6251.	1.8	1
342	Quasi-fivefold symmetric electron diffraction patterns due to multiple twinning in silicon thin films grown from hexamethyldisiloxane. Journal of Applied Crystallography, 2016, 49, 2226-2234.	4.5	1

#	Article	IF	CITATIONS
343	Molecular Beam Epitaxy of Germanium in the Atomic-Resolution Transmission Electron Microscope. Microscopy and Microanalysis, 2019, 25, 47-48.	0.4	1
344	In situ Photoluminescence Study of Plasma Effects on Passivation of Crystalline Silicon Coated with Aluminum Oxide. Physica Status Solidi (A) Applications and Materials Science, 2019, 216, 1800612.	1.8	1
345	Silicon Nanowire Solar Cells with μcâ€5i:H Absorbers for Radial Junction Devices. Physica Status Solidi (A) Applications and Materials Science, 2021, 218, 2100231.	1.8	1
346	In Situ Modulated PhotoLuminescence For Process Optimization Of Crystalline Silicon Passivation. , 2020, , .		1
347	Plasma-Enhanced Chemical Vapor Deposition in a Transmission Electron Microscope?. Microscopy and Microanalysis, 2021, 27, 25-26.	0.4	1
348	Bulk Defects and Hydrogenation Kinetics in Crystalline Silicon Solar Cells With Fired Passivating Contacts. IEEE Journal of Photovoltaics, 2022, 12, 711-721.	2.5	1
349	Triple Radial Junction Hydrogenated Amorphous Silicon Solar Cells with >2 V Open ircuit Voltage. Solar Rrl, 0, , 2200248.	5.8	1
350	Compton profiles of amorphous and hydrogenated amorphous silicon. Solid State Communications, 1997, 104, 193-197.	1.9	0
351	Trapping phenomena in intrinsic hydrogenated amorphous silicon like materials studied using current transient spectroscopies. Journal of Non-Crystalline Solids, 2006, 352, 1130-1133.	3.1	Ο
352	Fractional composition of large crystallite grains: A unique microstructural parameter to explain conduction behavior in single phase undoped microcrystalline silicon. Journal of Non-Crystalline Solids, 2008, 354, 2242-2247.	3.1	0
353	Low-temperature growth of nano-structured silicon thin films on ITO initiated by metal catalysts. Thin Solid Films, 2009, 517, 6405-6408.	1.8	0
354	(Invited) In-plane Silicon Nanowires for Field Effect Transistor Application. ECS Transactions, 2011, 37, 147-154.	0.5	0
355	Investigation of silicon heterojunction solar cells by photoluminescence under DC-bias. EPJ Photovoltaics, 2013, 4, 45106.	1.6	Ο
356	A modelling study of the performance of conventional diffused P/N junction and heterojunction solar cells at different temperatures. EPJ Photovoltaics, 2013, 4, 40101.	1.6	0
357	Modeling of Mueller Matrix Response from Diffracting Structures. Journal of Nanoscience and Nanotechnology, 2016, 16, 7805-7809.	0.9	Ο
358	Electrical characterization of low temperature plasma epitaxial Si grown on highly doped Si substrates. EPJ Photovoltaics, 2020, 11, 4.	1.6	0
359	Coupled Investigation of Contact Potential and Microstructure Evolution of Ultra-Thin AlOx for Crystalline Si Passivation. Nanomaterials, 2021, 11, 1803.	4.1	0
360	Formation of inverse cones in crystalline silicon by selective etching of amorphous regions resulting from epitaxial breakdown. Journal Physics D: Applied Physics, 2021, 54, 495103.	2.8	0

#	Article	IF	CITATIONS
361	Tapering-free monocrystalline Ge nanowires synthesized via plasma-assisted VLS using In and Sn catalysts. Nanotechnology, 2022, , .	2.6	о
362	In situ modulated photoluminescence study of the hydrogenation processes of tunnel oxide passivating contacts during plasma processes. Plasma Processes and Polymers, 0, , .	3.0	0